Journal of Hazardous Materials 199–200 (2012) 200–208

Contents lists available at SciVerse ScienceDirect

Journal of Hazardous Materials

journal homepage: www.elsevier.com/locate/jhazmat

TG–FTIR–MS (Evolved Gas Analysis) of bidi tobacco powder during combustion and pyrolysis

Tansir Ahamad, Saad M. Alshehri*

Department of Chemistry, King Saud University, P.O. Box 2455, Riyadh 11451, Saudi Arabia

ARTICLE INFO

Article history:
Received 31 May 2011
Received in revised form 12 October 2011
Accepted 28 October 2011
Available online 7 November 2011

Keywords:
Indian bidi
TG/FTIR/MS
Tobacco
Cancer
Nicotine

ABSTRACT

Bidi smoke, a complex mixture of toxic and carcinogens chemicals causes a large and growing number of premature deaths in South Asian countries especially in India and Bangladesh. The evolved products during the thermal degradation of bidi tobacco powder (BTP) have been measured by using TG–FTIR–MS technique. The results revealed that the main gases and volatile products released during the combustion and pyrolysis of BTP are CO, CO_2, NH_3, HCN, NO, isoprene, formaldehyde, acetaldehyde, acrolein, etc. Still others such as nicotine, phenol, polyaromatic hydrocarbon and some tobacco specific nitrosamines are contained in submicron sized solid particles that are suspended in Bidi smoke. The intensity or the quantity of evolved products is higher during the combustion than pyrolysis of BTP.

The evolved chemical data suggest that Bidi smoke is responsible for cancer of the throat, oral cavity, pharynx, larynx, lungs, esophagus, stomach, and liver.

1. Introduction

Bidis are small hand-rolled unfiltered cigarettes, very common in South Asian countries, seven or eight times more than cigarettes [1]. Bidi production does not need much technology and the workers do not wear protective clothes, gloves or masks. They are chronically exposed to tobacco flakes and dust via the cutaneous and nasopharyngeal routes. Hence, workers in a tobacco processing factory were monitored for chromosomal aberrations (CA) using peripheral blood lymphocytes as the test system and other side effects such as pain and cramps in shoulders, neck, back and lower abdomen. Although primarily an Indian product, but also exported abroad and have recently become popular in the United States, especially among young people [2]. In India alone, in 2010 smoking was the main case of about 930,000 adult premature deaths; of the dead, about 70% (90,000 women and 580,000 men) will be between the ages of 30 and 69 years [3]. Absolute number of deaths in this age group is rising by about 3% per year due to the population growth. Tobacco smoke is composed of a complex mixture of over 4000 chemicals resulting from pyrolysis [4]. Many of these chemicals exist in very small quantities just above the detection limits of sensitive toxicology assays, but many highly toxic chemicals are present in large measurable concentrations in tobacco smoke and are known to be involved in causing a variety of diseases. The particulate phase consists of tar (itself composed of many chemicals), nicotine, benzo(a)pyrene, and hundreds of other noxious compounds. A few examples of gases and volatile products in tobacco smoke are carbon monoxide, benzene, ammonia, dimethylnitrosamine, formaldehyde, hydrogen cyanide and acrolein [5–10]. Nair et al. identified carcinogenic tobacco specific nitrosamines from the smoke of bidis in concentrations similar to those of commercial cigarettes [11]. Bidis also deliver considerable amounts of carbon monoxide, resulting in increased blood carboxyhaemoglobin concentrations, main cause of bronchitis, tuberculosis, and respiratory diseases. The evolved HCN may affect the human respiratory system by its toxic effects on the cilia that line the respiratory tract [12]. In 1986, the International Agency for Research on Cancer (IARC) working group found that there is sufficient evidence that active tobacco smoking is carcinogenic for humans, and concluded that tobacco smoking caused cancers not only of the lung, but also of the lower urinary tract including the renal pelvis and bladder; upper aero-digestive tract including oral cavity, pharynx, larynx, and esophagus; and pancreas [13–16]. TG–FTIR–MS a powerful method has been used in previous studies to measure evolved gases during the thermal treatment of various substances [17–20]. This method offers the potential for the non-destructive, simultaneous, real-time measurement of multiple gas phase compounds in complex mixture. In the present study, we report the evolved gas analysis during the thermal degradation of bidi tobacco powder (BTP). The thermal degradation is in a helium and oxygen environment during pyrolysis and combustion respectively. The evolved volatile products were analyzed by thermogravimetric/Fourier transform infrared (TG–FTIR) and thermogravimetric/mass spectroscopy (TG–MS).

* Corresponding author. Tel.: +966 1 4675971; fax: +966 1 4674018.
E-mail address: alshehri@ksu.edu.sa (S.M. Alshehri).

0304-3894/$ – see front matter © 2011 Elsevier B.V. All rights reserved.
doi:10.1016/j.jhazmat.2011.10.090

Table 1
Composition of elements for the sample shown in Fig. 1 obtained from SEM/EDX.

Elements	BTP[a]		Pyrolysis residue		Combustion residue	
	wt.%	at.%	wt.%	at.%	wt.%	at.%
C K	47.93	63.29	18.34	22.93	4.75	8.24
O K	29.43	29.18	43.27	52.26	42.25	46.23
Mg K	1.25	1.00	9.51	8.28	9.28	7.95
Al K	1.20	0.92	2.30.	1.23	2.25	2.42
Si K	1.73	0.49	1.30	0.98	2.24	2.12
Cl K	2.62	1.84	0.00	0.00	0.00	0.00
S K	0.87	0.50	2.76	2.94	1.19	0.78
K K	3.31	1.99	8.62	6.13	5.64	5.49
Ca K	3.69	1.65	18.48	22.12	16.83	20.24
Fe K	1.13	0.74	2.34	2.46	1.68	0.63
Cd K	0.20	0.22	0.81	0.74	0.98	1.12
Hg K	0.10	0.14	0.28	0.42	0.32	0.54

[a] Bidi tobacco powder.

2. Experiments

2.1. Materials

The tested bidi was a popular Indian brand and was brought from an open market in New Delhi (India). A bidi consists of about 0.2–0.5 g of sun-dried and processed tobacco flakes, rolled in a tendu leaf (*Diospyros elanoxylon* or *Diospyros ebenum*) and held together by a cotton thread. The tendu leaf constitutes 60% of the weight of the bidi [21]. The tobacco rolled in bidi is different from that used in cigarettes and is referred to as *bidi tobacco* [22]. Dark and sun-dried bidi tobacco was crushed mechanically to obtain its powder. The particle size of the resulting powder was in the range of 100–300 μm. The SEM micrographs (scanning electron microscopy) of BTP are shown in Fig. 1 and the composition of elements (weight percentage and atom percentage) obtained from SEM/EDX is illustrated in Table 1.

2.2. Method

The TG–FTIR–MS analysis was performed using simultaneous thermogravimetry (STD 600 TA Instrument) coupled with FTIR (Bruker Tensor 27) and mass spectrometry (ThermoStar, Pfeiffer Vacuum). The analysis was performed under following helium and oxygen at 100 mL min^{-1}. The coupling systems between TG–FTIR and TG–MS were heated at 200 °C to prevent condensation of evolved gases and FTIR scanning range was from 400 to 4000 cm^{-1}. The mass spectrometer was operated at 70 eV. The m/z was carried out from 1 to 100 amu to determine which m/z has to be followed during the TG experiments. The ion curves close to the noise level were omitted. Finally, only the intensities of 25 selected ions (m/z = 12, 14, 15, 16, 17, 18, 20, 26, 27, 28, 30, 31, 32, 40, 42, 43, 44, 45, 54, 56, 58, 68, 78, 94 and 108) were monitored with the thermogravimetric parameters. The number of gaseous species released during the thermal degradation of BTP is significant therefore for the purpose of this study, a sample of approximately 20–30 mg was heated in helium and oxygen at 10, 20, 30, and 50 °C min^{-1}, first to 100 °C to dry the sample for 2 min, and then to 950 °C for thermal degradation. The small sample size used in this work ensured that temperature gradients within the sample were minimized.

3. Results and discussion

3.1. TG measurements of bidi tobacco powder (BTP)

The thermogravimetric (TG) and differential thermogravimetric (DTG) curves during pyrolysis and combustion of BTP at a heating rate 30 °C min^{-1} are shown in Figs. 2 and 3 respectively.

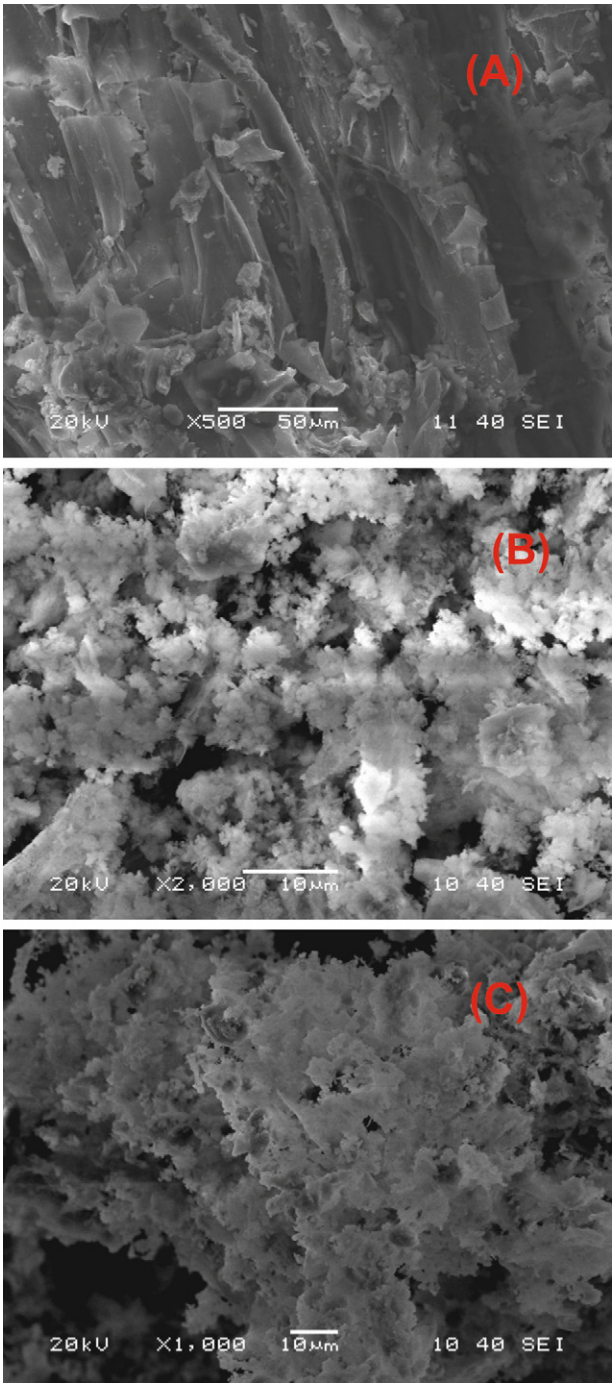

Fig. 1. SEM micrographs of TBP: (A) crushed BTP, (B) residue during combustion and (c) residue during pyrolysis.

Based on DTG profile, pyrolysis process can be subdivided into four stages. The first stage is a 5.96% weight loss for drying the sample (below 150 °C). Surface moisture and inherent moisture are emitted in this stage. The second stage is fast thermal decomposition for BTP between 200 °C and 400 °C; most of the weight loss (about 42.51 wt.% of the total weight of original samples) occurs during this stage, corresponds to the main step of tobacco powder degradation in to volatile product. There are two peaks in the DTG curve (weight loss rate) at this stage: the maximum weight loss rate was occurred at 344.7 °C, while the temperature at secondary peak was 296 °C with 8.63% weight loss per minute. The last stage in pyrolysis is further cracking process of the tobacco powder residue in

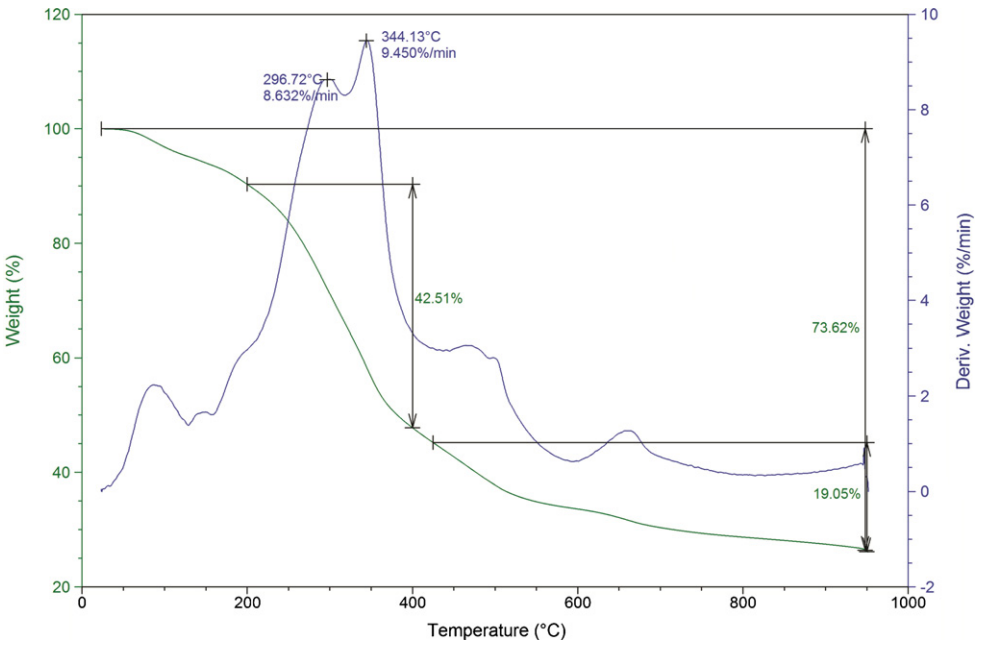

Fig. 2. TG/DTG of TBP during pyrolysis.

a wider temperature range, from 425 °C to the end of this experiment (950 °C); about 19 wt.% of the total weight loss at a lower rate in this stage, and the total weight loss of 73.5 wt.% was discovered at 950 °C.

The combustion of bidi powder at low temperature up to 400 °C is similar to that of pyrolysis and found to be 43.10% of the total weight lost at the temperature range between 200 °C and 400 °C. The weight loss rate reaches its maximum value at 469 °C and about 40.42% min^{-1} weight loss was observed at this stage. After 500 °C, the molecules of BTP start to crack. The total weight loss of 86.53 wt.% was discovered at 950 °C in BTP combustion. The remaining solid products from pyrolysis and combustion contain char, ash and unchanged biomass material. The SEM micrographs of the tobacco residue are given in Fig. 1 and the composition of elements (weight percentage and atom percentage) obtained from SEM/EDX analyses are illustrated in Table 1. The metals, such as nickel, lead, cobalt and cadmium found in residue of BTP after combustion and pyrolysis are cancer-causing ingredients, inhaling them in tobacco smoke is worse, because they are easily absorbed by the lungs [23–25].

3.2. Pyrolysis and combustion kinetics

The pyrolysis and combustion of BTP could be divided into four non-interacting weight loss stage on the basis of DTG profiles, which can be described by four independent parallels first order reactions [25]. The first order reaction based Arrhenius theory is

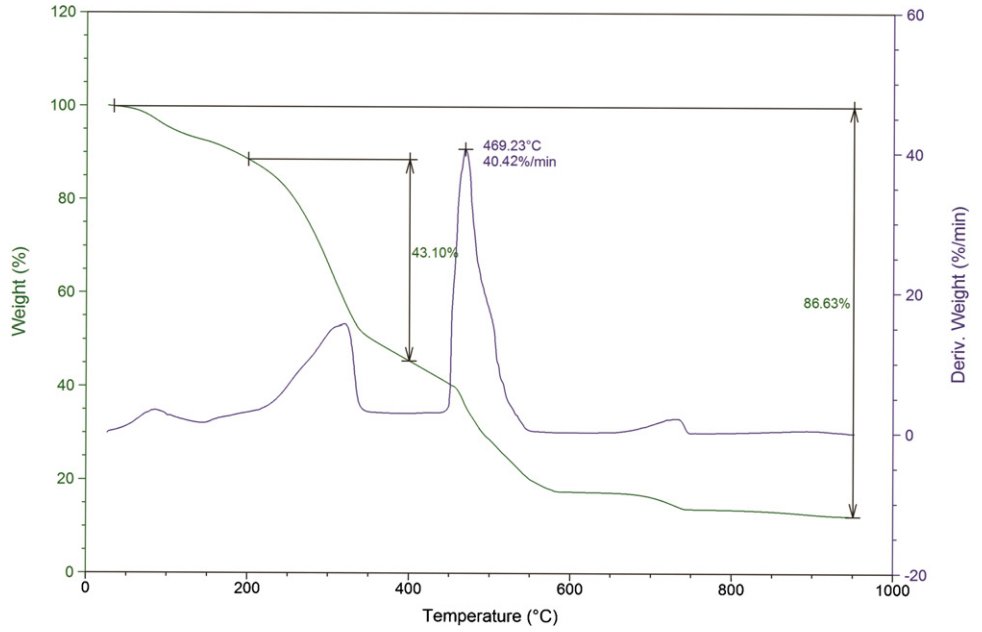

Fig. 3. TG/DTG of TBP during combustion.

Table 2
First order kinetic parameters (activation energy and Arrhenius pre-exponential factors and coefficient of determination) of the BTP during pyrolysis and combustion.

Temperature stage	Activation energy (kJ mol^{-1})	Pre-exponential factor (s^{-1})	R^2
Pyrolysis at second stage	45.4	3.61E+002	0.851
Combustion at second stage	62.45	3.52E+001	0.913

commonly assumed in the kinetic analysis during combustion and pyrolysis.

$$k = A\exp\left(-\frac{E}{RT}\right) \quad (1)$$

where k is constant of reaction rate, T is thermodynamic temperature (K), R is universal gas constant ($R = 8.314\,\mathrm{J\,mol^{-1}\,K^{-1}}$), E is activation energy and A is a pre-exponential factor. The rate of decomposition may be expressed by:

$$\frac{d\alpha}{dt} = k(1-x) \quad (2)$$

where α is mass loss fraction and defined as:

$$\alpha = \frac{m_0 - m_t}{m_0 - m_f}$$

where m_0 is the initial mass sample, m_t is mass sample at t time during thermal degradation and m_f is the final mass when experiment finished. Taking into account that temperature is a function of time and increase with constant heating rate β the following expression derives:

$$T = \beta t + T_0 \quad (3)$$

Differentiating the above correlation, it derives:

$$dT = \beta dt$$

Eq. (2) could be written as

$$\frac{d\alpha}{1-\alpha} = \frac{k}{\beta}dT \quad (4)$$

An integration function of above Eq. (4) is shown below

$$g(\alpha) = \int_0^{\alpha}\frac{d\alpha}{dt} = \frac{A}{\beta}\int_0^{t}\exp\left(-\frac{E}{RT}\right)\,dT \quad (5)$$

where $g(\alpha) = -\ln(1-\alpha)$.Eq. (5) is integrated by using Caots–Redfern method:

$$\ln\frac{g(\alpha)}{T^2} = \ln\left(\frac{AR}{\beta E}\left[1-\frac{2RT}{E}\right]\right) - \frac{E}{RT} \quad (6)$$

where $g(\alpha)$ is the kinetic mechanism function in integral form.

As the term of $2RT/E$ can be neglected since it is much less than 1, Eq. (6) could be simplified as

$$ln\frac{g(\alpha)}{T^2} = \ln\left(\frac{AR}{\beta E}\right) - \frac{E}{R}\frac{1}{T} \quad (7)$$

The term of $\ln(g(\alpha)/T^2)$ varies linearly with $1/T$ at a slope $-E/R$. Meanwhile, the intercept of the line with y-axis is related to the pre-exponential factor A. Both the activation energy E and pre-exponential factor A can be determined by the slope and intercept of the line and presented in Table 2.

3.3. FTIR analysis of evolved gas

The infrared Gram–Schmidt reconstructs based on vector analysis of the acquired interferograms allow plots of the total evolved gases detected by the spectrometer to be generated (Fig. 4). The detector signal has been plotted as a function of sample temperature and qualitatively approximates DTG curves recorded during the TG experiments performed under different controlled conditions. It should be noted that the peaks in the Gram–Schmidt plot are shifted to higher temperatures than the corresponding DTG curve; this is due to the delay time between the gas generation and its detection in the FTIR equipment. In the Gram–Schmidt plot of BTP during the pyrolysis, the second peak is big, when compared with second peak during combustion, suggesting that the amount of the evolved gases in this stage is large and with high infrared extinction coefficients. In contrast, the third degradation stage seems to be composed of a small amount of evolved gases with low infrared extinction coefficients. The peak observed in the Gram–Schmidt plot during combustion in big intensity suggests that the amount of evolved gas in this stage is very high and with very high infrared extinction coefficients. Fig. 5 shows 3D FTIR spectra for the gases produced from thermal degradation and Fig. 6 shows the FTIR spectrograms at 270 °C temperature during pyrolysis and combustion of BTP. The temperature dependence of intensity agrees well with the temperature dependence of DTG curve, and the intensity of gas emission reaches its maximum at 270 °C, which is the same temperature of the maximum loss rate during pyrolysis and combustion. The main gases released during the pyrolysis of BTP are H_2O, CO_2, CO, NH_3, HCN, NO, NO_2 and some organic volatile compounds such as aldehydes (propionaldehyde, acetaldehyde and formaldehyde) and acids (C=O), alcohols and phenols (C–O), alkanes (C–C), alkenes (C=C) and aromatic hydrocarbon. The emission of water follows two steps. At first, the absorbed water is released out by evaporation. Secondly, when the temperature reaches 200 °C, water was generated by the cleavage of aliphatic hydroxyl groups and confirmed by the appearance of bands at 3550–3640 cm^{-1}. The gases emission was mainly concentrated between 200 and 700 °C, which is in agreement with the thermogravimetric data. The presence of CO_2 and CO was confirmed by the appearance of band at 2326 cm^{-1} and 2176 cm^{-1} respectively [26]. Absorption bands at 2981 and 2889 cm^{-1}, related to C–C stretching for aliphatic compounds and a band at 1634 cm^{-1} due to C=C stretching of unsaturated group (alkene) were also observed. Fig. 7, the FTIR spectrum of evolved gases during combustion and pyrolysis shows the production of aromatic hydrocarbons at higher temperature (up to 500 °C) was confirmed by the appearance of band at 3011 and 845 cm^{-1}. Another bands at 3474 cm^{-1} and 1264 cm^{-1} which is related to N–H stretching vibration and C–N stretching vibration of NH_3 and amines respectively produced by the cleavage of Nicotine and tobacco-specific nitrosamines. In the similar manner, the presences of carbonyl groups (formaldehydes, acetaldehyde and propionaldehyde) in the evolved gases during the pyrolysis of BTP were confirmed by the appearance of bands between 1680 and 1750 cm^{-1}. Tobacco smoke contains also high concentrations of toxic aldehydes [27]. The most abundant aldehyde in tobacco smoke is acetaldehyde, and its concentration in tobacco smoke is 1000 times greater than those of polycyclic aromatic hydrocarbons and tobacco-specific nitrosamines. Tobacco smoking is one of the strongest risk factors not only for lung cancer but also for cancers of the upper gastrointestinal tract. Acetaldehyde has been shown to dissolve into the saliva during smoking and become a local carcinogen in the human upper digestive tract. Cysteine can bind to acetaldehyde and eliminate its toxicity.

The emission of phenols and cresols was confirmed by the appearance of absorption peaks in the range 3526–3613 cm^{-1} corresponding to O–H stretching and another peaks at 1108 cm^{-1}, 1023 cm^{-1} were observed corresponding to C–O and O–H respectively.

The evolved gases and volatile products during the combustion of BTP are similar to the product evolved during the pyrolysis of BTP. It was observed that the intensities of CO_2, CO, H_2O, etc. were very high when compared with their intensities during pyrolysis, attributed to the oxidation of decomposition product. The

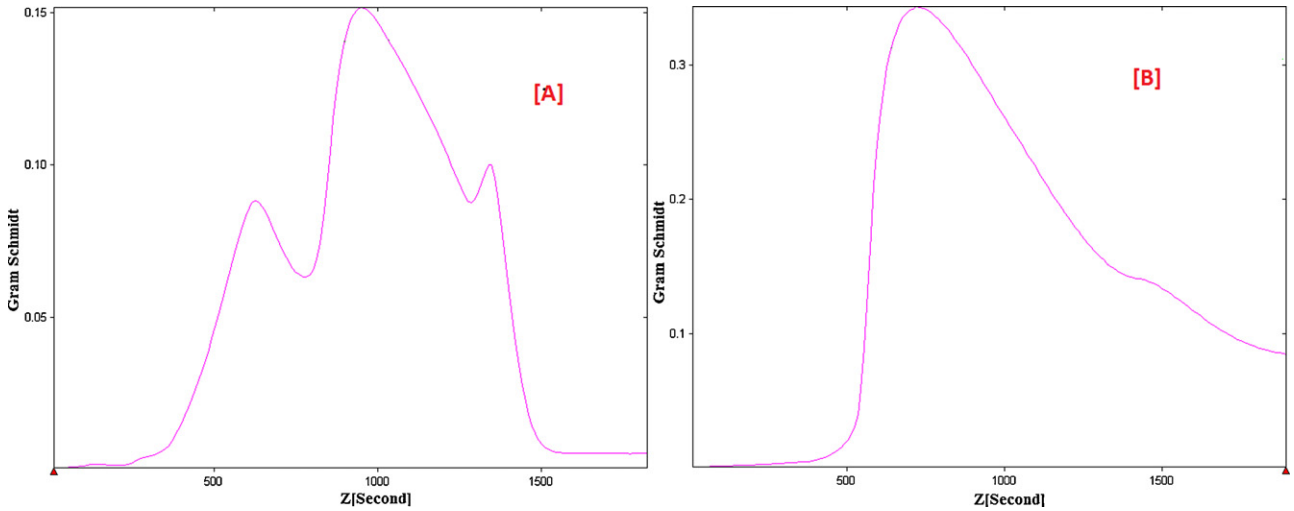

Fig. 4. Gram–Schmidt plot during thermal degradation: (a) pyrolysis and (b) combustion.

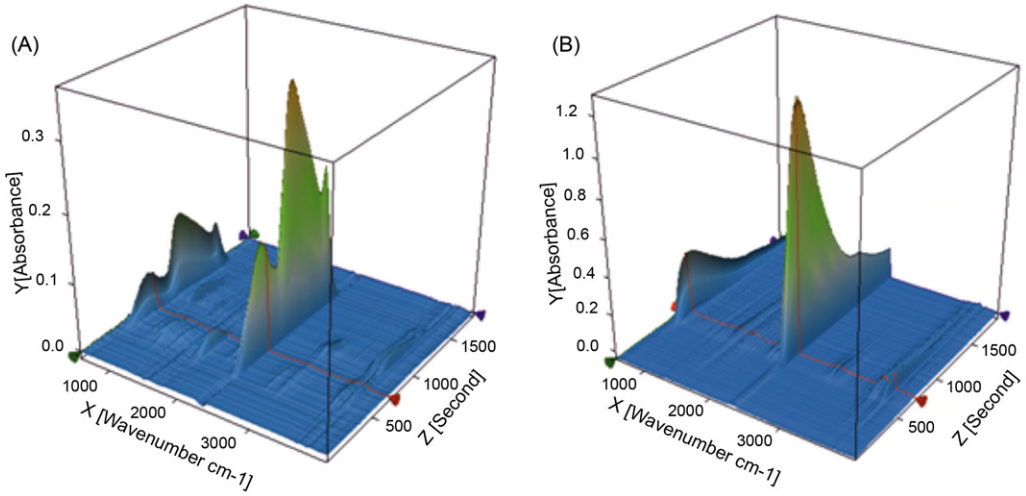

Fig. 5. 3D FTIR plot during thermal degradation: (a) pyrolysis and (b) combustion.

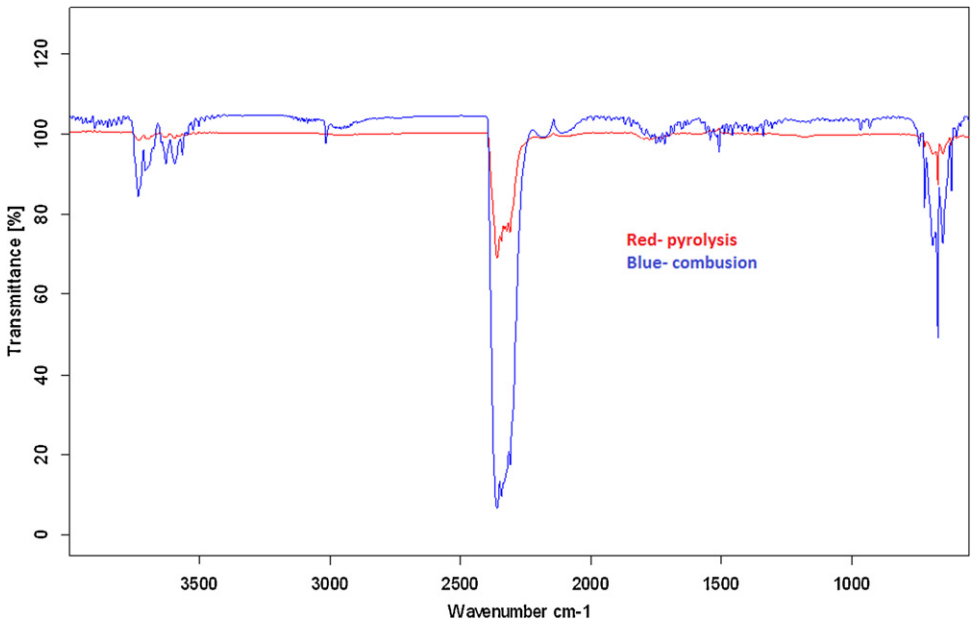

Fig. 6. Spectrograms during pyrolysis and combustion of BTP at 270 °C.

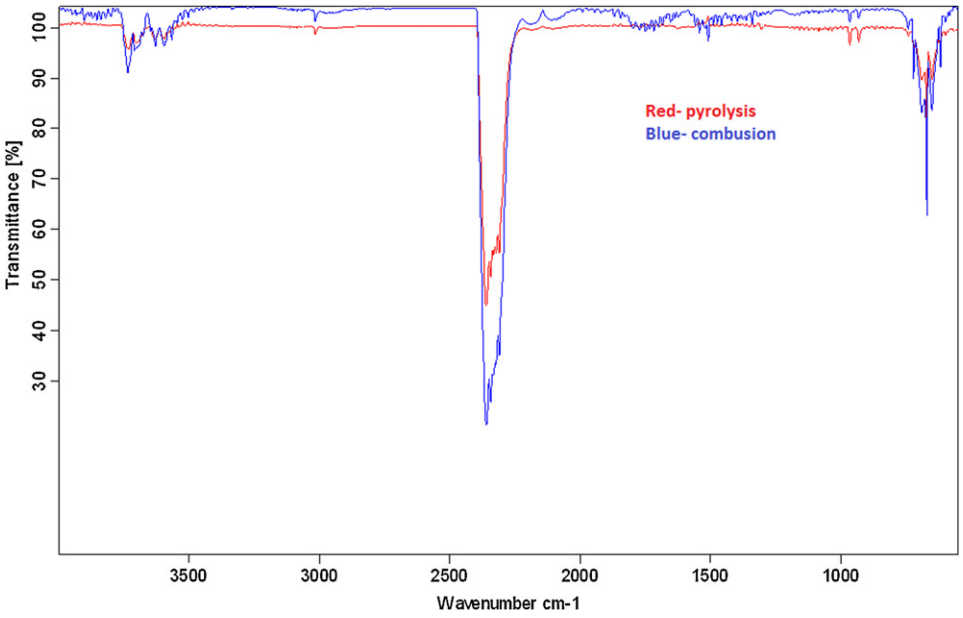

Fig. 7. Spectrograms during pyrolysis and combustion of BTP at 500 °C.

main evolved products obtained at 270 °C were H_2O, CO_2, CO, NH_3, HCN, NO, NO_2, formaldehyde, acetaldehyde, alkans, alkenes, aromatic hydrocarbons, amines, phenols, cresols, etc. [28]. Although some interesting results have been provided by the FTIR analysis, this technique has two main drawbacks. First, as observed on 3D plot of the FTIR spectra, a strong IR signal caused by absorption of H_2O appears during the pyrolysis, which can hide the detection of some gases. Secondly, there were gases released during the thermal decomposition, which were undetectable with FTIR such as H_2 and Cl_2. In order to follow all main gaseous products, further investigation was conducted using the coupling TG–MS.

3.4. Evolved gas analysis with MS

The evolved products during the thermal degradation of BTP were determined by thermogravimetry coupled to a mass spectrometer and are shown in Fig. 8a–j. The release of carbon dioxide during this degradation stage was confirmed by a fragment at m/z 44 (CO_2^+) (Fig. 8a), 28 (CO^+), and 45 ($C^{13}O_2$) it is also supported by FTIR data where carbon dioxide has been observed in all three stages, but it is much more pronounced in the second step of the BTP combustion [29]. The releasing of water begins at 100 °C and shows fragments at m/z 18 in the first and second degradation stage during pyrolysis and combustion of BTP.

In Fig. 8a, the peaks at m/z 27 which appear with strong intensity in the second degradation step between 250 and 500 °C can be assigned to HCN or $C_2H_3^+$ ions. While the intensity of this fragment is very low during the pyrolysis of BTP. HCN may affect the human respiratory system by its toxic effects on the cilia that line the respiratory tract. At the same time, HCN may cross the placenta and have toxic effect on growing fetus and cause nerve damage [30].

The mass per charge ratio, $m/z = 28$ corresponds mainly to CO, C_2H_4, and N_2. All the three can be expected from BTP keeping in mind the high amount of oxygen containing molecules in the plant materials, m/z 28 is due mainly to CO [31]. This is in agreement with the TG–FTIR spectra. The release of other volatile products during second stage degradation show fragment at m/z 68 and 54 with 42 due to the presence of isoprene and butadiene with propane shown in Fig. 8c and 8 respectively [32]. Isoprene and butadiene caused a macrocytic anemia; induced increases in sister chromatid exchanges in bone marrow cells and in levels of micronucleated erythrocytes in peripheral blood; and produced degeneration of the olfactory epithelium, forestomach epithelial hyperplasia, testicular atrophy and carcinogenic effect on liver, lung, harderian [33]. In Fig. 8e–f some additional peaks were observed at m/z 78, 94 and 108, which can be assigned to benzene, phenol, and *o*-cresol, *m*-cresol, *p*-cresol fragments respectively [34,35]. It is well-established that benzene can cause cancer, particularly leukaemia. It could account for between a tenth and a half of the deaths from leukaemia caused by smoking [36].

The MS fragments at for propionaldehyde ($m/z = 58$), acetaldehyde ($m/z = 44$) and formaldehyde ($m/z = 30$) show intensity at 270 °C during the combustion while during the pyrolysis the intensity is continually increased and are shown in Fig. 8g and h [37,38]. The m/z 29 corresponds mainly to ions CHO^+ and $C_2H_5^+$. Former is characteristic to aldehydes, most abundant fragment of formaldehyde, but other organic compounds can also produce it. Latter is a low-abundance fragment of several compounds containing $-C_2H_5$. The releasing of gas contributing to $m/z = 17$ (ammonia) fragment happened at a large number of temperature, First emission occurs between 200 and 300 °C, and second release appears between 400 and 500 °C as in Fig. 8i [39]. Another nitrogen rich product was observed at $m/z = 74$ (dimethylnitrosamine) [40], that can directly damage DNA, like polycyclic aromatic hydrocarbons (PAHs). Nitrosamines are found in small amounts in food, but tobacco products, including those that are chewed rather than smoked, are by far our largest source of exposure to these chemicals. Even though they are found in relatively small amounts in tobacco, they are very strong cancer-causing chemicals [41]. Finally in Fig. 8j, acrolein ($m/z = 56$) [42], a gas with an intensely irritating smell and is one of the most abundant chemicals in BTP smoke belongs to the same group of chemicals as formaldehyde and acetaldehyde, both of which can cause cancer [43]. Until now, it was not clear if acrolein causes cancer as well, but recent experiments suggest that it can. We now know that acrolein can cause DNA damage that is similar to the damage seen in lung cancer patients. Since smoke contains up to 1000 times more acrolein than other DNA-damaging chemicals, it could be a major cause of lung cancer. Acrolein also stops our cells from repairing DNA damage, like arsenic and cadmium. Like hydrogen cyanide, it kills the hairs that normally clean our lungs of other toxins [44]. The MS spectrum of products released during the pyrolysis of BTP is

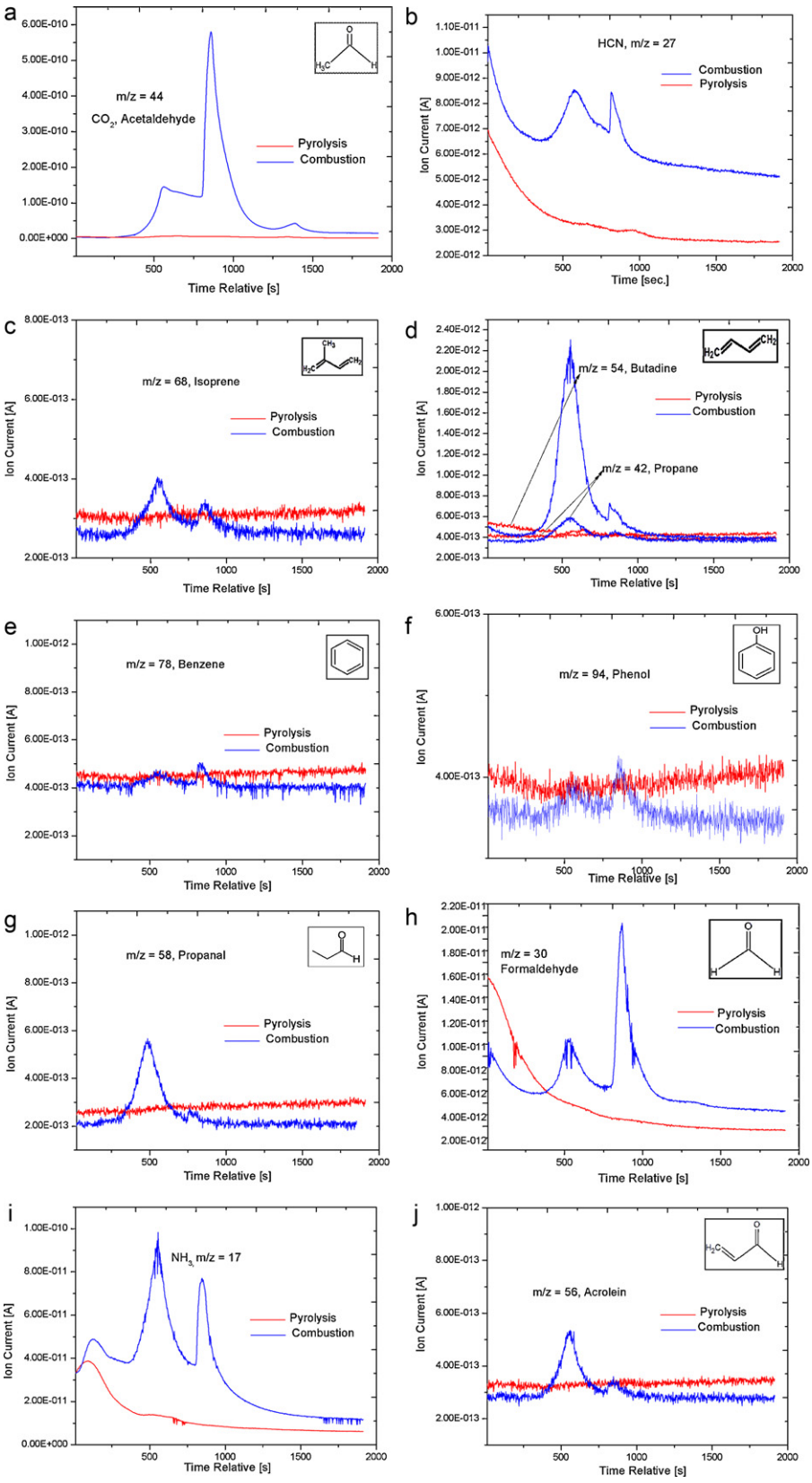

Fig. 8. (a) Single ion current curves of $m/z = 27$ during thermal degradation of BTP. (b) Single ion current curves of $m/z = 44$ during thermal degradation of BTP. (c) Single ion current curves of $m/z = 68$ during thermal degradation of BTP. (d) Single ion current curves of $m/z = 54$ and $m/z = 44$ during thermal degradation of BTP. (e) Single ion current curves of $m/z = 78$ during thermal degradation of BTP. (f) Single ion current curves of $m/z = 94$ during thermal degradation of BTP. (g) Single ion current curves of $m/z = 58$ during thermal degradation of BTP. (h). Single ion current curves of $m/z = 30$ during thermal degradation of BTP. (i) Single ion current curves of $m/z = 17$ during thermal degradation of BTP. (j) Single ion current curves of $m/z = 56$ during thermal degradation of BTP.

completely different than combustion and the quantity of evolved product is very low when comparing with corresponding combustion product.

Thus, the FTIR analysis and the mass spectrometry have advantages and disadvantages. However, using information provided by each of them, it is possible to have an identification of the gases emitted by degradation of BTP during pyrolysis and combustion.

4. Conclusion

The products evolved during the combustion and pyrolysis were studies by using TG–FTIR–MS technique. The main gases and volatile products released during the combustion and pyrolysis of BTP are CO, CO_2, NH_3, HCN, NO, isoprene, formaldehyde, acetaldehyde, acrolein, etc. Still others such as nicotine, phenol, polyaromatic hydrocarbon and some tobacco specific nitrosamines are contained in submicron sized solid particles that are suspended in bidi smoke. Last but not least, the data reported here are in line with the human data which suggest a correlation between bidi smoking and cancers. According to a recent systematic evaluation tobacco is a potent multisite carcinogenic with a worldwide impact, causing cancers of lung, upper aero-digestive tract (oral cavity, nasal cavity, nasal sinuses, pharynx, larynx and oesophahus), pancreas, stomach, liver, lower urinary cervix and myeloid leukaemia. Therefore, bidi smoking is very harmful and causes a large and growing number of premature deaths in India and other countries.

Acknowledgement

We are gratefully acknowledged "The Deanship of Scientific Research, Research Center, College of Science," King Saud University, Kingdom of Saudi Arabia to support this work.

References

[1] Tobacco or Health: A Global Status Report, World Health Organization, Geneva, 1997.
[2] L.M. Jennifer, B.P. Wallace, Bidis-hand-rolled, Indian cigarettes: effects on physiological biochemical and subjective measures, Pharmacol. Biochem. Behav. 72 (2002) 443–447.
[3] P. Jha, P.B. Jacob, V. Gajalakshmi, P.C. Gupta, N. Dhingra, R. Kumar, D.N. Sinha, R.P. Dikshit, D.K. Parida, R. Kamadod, J. Boreham, R. Peto, A nationally representative case–control study of smoking and death in India, N. Engl. J. Med. 13 (2008) 1137–1147.
[4] X. Bi, G. Sheng, Y. Feng, J. Fu, J. Xie, Gas- and particulate specific tracer and toxic organic compounds in environmental tobacco smoke, Chemosphere 61 (2005) 1512–1522.
[5] A. Rodgman, R.G. Green, Toxic chemicals in cigarette mainstream smoke – hazards and hoopla, Beitr. Tabakforsch. 20 (2003) 481–554.
[6] A. Rodgman, T.A. Perfetti, The Chemical Components of Tobacco and Tobacco Smoke, CRC Press, Taylor and Francis Group, Boca Raton, Florida, 2008.
[7] C. Meredith, F. Cunningham, E.D. Massey, Risk assessment paradigms with tobacco smoke constituents, Toxicology 253 (2008) 13.
[8] J. Fowles, E. Dybing, Application of toxicological risk assessment principles to the chemical constituents of cigarette smoke, Tob. Control 12 (2003) 424–430.
[9] S. Mizusaki, H. Okamoto, A. Akiyama, Y. Fukuhara, Relation between chemical constituents of tobacco and mutagenic activity of cigarette smoke condensate, Mutat. Res. 48 (1977) 319–326.
[10] W. Tarora, K. Torikai, H. Takahashi, Studies on the generation of carbonyl compounds in tobacco smoke, Paper presented at 57th Tobacco Science Research Conference, Norfolk, VA, USA, Program Booklet and Abstracts, 2003.
[11] J. Nair, S.S. Pakhale, S.V. Bhide, Carcinogenic tobacco-specific nitrosamines in Indian tobacco products, Food Chem. Toxicol. 23 (5) (1989) 1–3.
[12] R.R. Baker, E.D. Massey, G. Smith, An overview of the effects of tobacco ingredients on smoke chemistry and toxicity, Food Chem. Toxicol. 42 (2004) 53–83.
[13] World Health Organization, International Agency for Research on Cancer, IARC Monographs on the Evaluation of Carcinogenic Risks to Humans. Tobacco Smoking and Involuntary Smoking, vol. 83, Lyon, IARC, 2004.
[14] P. Vineis, M. Alavanja, P. Buffler, Tobacco and cancer: recent epidemiological evidence, J. Natl. Cancer Inst. 96 (2004) 99–106.
[15] US National Cancer Institute, Risks Associated with Smoking Cigarettes with Low Machine-Measured Yields of Tar and Nicotine, Smoking and Tobacco Control, Monograph 13, October 2001.
[16] R. Peto, S. Darby, H. Deo, P. Silcocks, E. Whitley, R. Doll, Smoking cessation and lung cancer in the UK since 1950: combination of national statistics with two case–control studies, BMJ 321 (2000) 323–329.
[17] T. Ahamad, S.M. Alshehri, Thermal degradation and evolved gas analysis of thiourea-formaldehyde resin (TFR) during pyrolysis and combustion, J. Therm. Anal. Calorim. (2010), doi:10.1007/s10973-011-1882-1.
[18] X. Jiang, C. Li, Y. Chi, J. Yan, TG–FTIR study on urea-formaldehyde resin residue during pyrolysis and combustion, J. Hazard. Mater. 173 (2010) 205–210.
[19] J. Madarasz, S. Kaneko, M. Okuya, G. Pokol, Comparative evolved gas analyses of crystalline and amorphous titanium(IV)oxo-hydroxo-acetylacetonates by TG–FTIR and TG/DTA–MS, Thermochim. Acta 489 (2009) 37–44.
[20] J. Madarasz, P.P. Varga, G. Pokol, Evolved gas analyses (TG/DTA–MS and TG–FTIR) on dehydration and pyrolysis of magnesium nitrate hexahydrate in air and nitrogen, J. Anal. Appl. Pyrol. 79 (2007) 475–478.
[21] C. Celebucki, D.M. Turner-Bowker, G. Connolly, H.K. Koh, Bidi use among urban youth Massachusetts, MMWR 48 (1999) 796–799.
[22] Centers for Disease Control and Prevention, Tobacco use among middle and high school students United States, 1999, MMWR (2000) 49–53.
[23] C.A. Adamu, P.F. Bell, C.L. Mulchi, R.L. Chaney, Residual metal levels in soils and leaf accumulations in tobacco a decade following farmland application of municipal sludge, Environ. Pollut. 56 (1989) 113–126.
[24] C.A. Bache, D.J. Lisk, G.J. Doss, D. Hoffmann, J.D. Adams, Cadmium and nickel in mainstream particulates of cigarettes containing tobacco grown on a low cadmium soil–sludge mixture, J. Toxicol. Reprod. Health 16 (1985) 547–552.
[25] V. Krivan, G. Schneider, H. Baumann, U. Reus, Multi-element analysis of tobacco smoke condensate, Fresenius J. Anal. Chem. 348 (1994) 218–225.
[26] P.L. Gendreau, F. Vitaro, The unbearable lightness of "light" cigarettes – a comparison of smoke yields in six varieties of Canadian "light" cigarettes, Can. J. Public Health 96 (2005) 167–172.
[27] O. Laakso, M. Haapala, T. Kuitunen, J.J. Himberg, Screening of exhaled breath by low-resolution multicomponent FTIR spectrometry in patients attending emergency departments, J. Anal. Toxicol. 28 (2004) 111–117.
[28] R. Cueto, W.A. Pryor, Cigarette-smoke chemistry conversion of nitric-oxide to nitrogen-dioxide and reactions of nitrogen-oxides with other smoke components as studied by Fourier-transform infrared spectroscopy, Vibr. Spectrosc. 7 (1994) 97–111.
[29] R.R. Baker, D.P. Robinson, Tobacco combustion – the last ten years, Rec. Adv. Tob. Sci. 16 (1990) 3–101.
[30] J.D. Jonathan, I. Pendlebury, J.A. Richard, B. Shehr, J. Kathleen, M. Jennifer, Schneider, U. Shabih, Respiratory control in neonatal rats exposed to prenatal cigarette smoke, Am. J. Respir. Crit. Care Med. 177 (2008) 1255–1261.
[31] J.I. Seeman, S.W. Laffoon, A.J. Kassman, Evaluation of relationships between mainstream smoke acetaldehyde and tar and carbon monoxide yields in tobacco smoke and reducing sugars in tobacco blends of U.S. commercial cigarettes, Inhal. Toxicol. 15 (2003) 373–395.
[32] G. Vilcins, Determination of ethylene and isoprene in the gas phase of cigarette smoke by infrared spectroscopy, Beitr. Tabakforsch. 8 (1975) 181–185.
[33] R.F. Severson, M.E. Snook, R.F. Arrendale, Gas chromatographic quantitation of polynuclear aromatic hydrocarbons in tobacco smoke: analytic laboratory methods, Anal. Chem. 48 (1976) 1866–1872.
[34] S. Li, R.M. Olegario, J.L. Banyasz, K.H. Shafer, Gas chromatography–mass spectrometry analysis of polycyclic aromatic hydrocarbons in single puff of cigarette smoke, J. Anal. Appl. Pyrol. 66 (2003) 156–163.
[35] T. Adam, S. Mitschke, T. Streibel, R.R. Baker, R. Zimmermann, Puff-by-puff resolved characterisation of cigarette mainstream smoke by single photon ionisation (SPI)–time of flight mass spectrometry (TOFMS): comparison of the 2R4F research cigarette and pure Burley, Virginia Oriental and Maryland tobacco cigarettes, Anal. Chim. Acta 572 (2006) 219–229.
[36] L. Hao, Z. Lizhong, Pollution patterns of polycyclic aromatic hydrocarbons in tobacco smoke, J. Hazard. Mater. 139 (2007) 193–198.
[37] S. Li., J.L. Banyasz, M.E. Parrish, J. Lyons-Hart, K.H. Shafer, Formaldehyde in the gas phase of mainstream cigarette smoke, J. Anal. Appl. Pyrol. 65 (2002) 137–145.
[38] M.E. Parrish, C.N. Harward, Measurement of formaldehyde in a single puff of cigarette smoke using tunable diode laser infrared spectroscopy, Appl. Spectrosc. 54 (2000) 1665–1677.
[39] T. Adam, T. Ferge, S. Mitschke, T. Streibel, R.R. Baker, R. Zimmermann, Discrimination of three tobacco types (Burley, Virginia and Oriental) by pyrolysis single photon ionisation–time-of-flight mass spectrometry and advanced statistical methods, Anal. Bioanal. Chem. 381 (2005) 487–499.
[40] S. Mitschke, T. Adam, T. Streibel, R.R. Baker, R. Zimmermann, Application of time-of-flight mass spectrometry with laser-based photoionization methods for time-resolved on-line analysis of mainstream cigarette smoke, Anal. Chem. 77 (2005) 2288–2296.
[41] R. Peto, S. Darby, H. Deo, Smoking, smoking cessation, and lung cancer in the UK since 1950: combination of national statistics with two case–control studies, BMJ 321 (2000) 323–329.
[42] T. Adam, T. Streibel, S. Mitschke, F. Mühlberger, R.R. Baker, R. Zimmermann, Application of time-of-flight mass spectrometry with laser-based photoionization methods for analytical pyrolysis of PVC and tobacco, J. Anal. Appl. Pyrol. 74 (2005) 454–464.

[43] Office of the US Surgeon General, The Health Consequences of Smoking: Cancer: A Report of the Surgeon General, Centers for Disease Control and Prevention (CDC), Office on Smoking and Health, 1982, http://profiles.nlm.nih.gov/NN/B/C/D/W/ (accessed 28.10.10).

[44] K.M. Torrence, R.L. McDaniel, D.A. Self, M.J. Chang, Slurry sampling for the determination of arsenic, cadmium, and lead in mainstream cigarette smoke condensate by graphite furnace-atomic absorption spectrometry and inductively coupled plasma-mass spectrometry, Anal. Bioanal. Chem. 372 (2002) 723–731.